Received: 8 August 2021 | Revised: 14 October 2021 | Accepted: 17 October 2021 | Published online: 13 December 2021

RESEARCH ARTICLE

Journal of Computational and Cognitive Engineering
2022, Vol. 1(2) 74–82
DOI: 10.47852/bonviewJCCE2022010101

BON VIEW PUBLISHING

Reliability and Performance Analysis of a Series-Parallel System Using Gumbel–Hougaard Family Copula

Anas Sani Maihulla[1,2], Ibrahim Yusuf[2,*] and Saminu I. Bala[2]

[1]Department of Mathematics, Sokoto State University, Nigeria and [2]Department of Mathematical Sciences, Bayero University, Kano, Nigeria

Abstract: This research looks into the reliability metrics that are used to assess the strength of a solar system's serial system, which is made up of four subsystems. Each subsystem consists of two parallel active components: two out of two photo-voltaic panels, one of two charge controllers, two of two batteries, and one of two inverters. Both the charge controller and the inverter have two human operators or switches. The Gumbel–Hougaard copula family was used to produce formulations of system dependability metrics such as reliability, mean time to failure (MTTF), availability, and profit function. Numerical examples are presented to show the obtained results and to investigate the impact of various system characteristics. The new study might help homes overcome some of the problems experienced by electric generation systems operating in hostile locations or under adverse weather conditions. A new model was developed, and solar photovoltaic system's subsystems were analyzed in order to identify the most essential component. It was also indicated how to improve the system.

Keywords: strength; parallel; reliability; subsystem; availability; switch

1. Introduction

System reliability is a measure of how well a system performs under unfavorable situations. According to the specifications, most complex systems are made up of components and subsystems that are linked in series, parallel, standby, or a mixture of these. The phrases dependable and dependability are used in social, political, commercial, and technological settings to express faith/trust in a person, firm, or piece of equipment. A study of a photovoltaic system can help users make timely choices to guarantee the system's good functioning. As a consequence of operational research in the framework of military studies, the subject of dependability theory developed. Since antiquity, the terms "reliable" and "reliability" have been used interchangeably. In reality, they are frequently employed to illustrate the efficacy of a person or a piece of mechanical equipment in social, political, economic, and practical sectors. Later in 1950, the word "reliability" was given a mathematical structure in conjunction with its scientific use for military reasons. Because of the relevance of dependability theory, it was developed in the Western world. Scholars will find the history of dependability technology development in India to be both interesting and thrilling. Almost all of our everyday issues are impacted by dependability theory. Power, transportation, medical services, steel, and communication networks are just a few examples of systems whose dependability has a direct impact on society as a whole. According to the history of modern engineering, system failures can occur in any discipline.

Reliability analysis of the engineering systems using intuitionistic fuzzy set theory was studied by Garg et al. (2013). Fashina et al. (2018) carried out the study on the status quo of rural and renewable energy development in Liberia: policy and implementation. Quiles et al. (2020) study the accurate sizing of residential stand-alone photovoltaic systems considering system reliability. Rengasamy et al. (2020) study motivation for incorporation of microgrid technology in rooftop solar photovoltaic deployment to enhance energy economics. Salah & Fashina (2019) carried out the design of a hybrid solar photovoltaic system for Gollis University's administrative block, Somaliland. Uswarman and Rushdi (2021) conducted the reliability evaluation of rooftop solar photovoltaic using coherent threshold systems. Patelli and Beer (2017) study the reliability analysis on complex systems with common cause failure safety, reliability, risk, resilience and sustainability of structures and infrastructure. Sayed et al. (2019) analyze the reliability, availability, and maintainability analysis for grid-connected solar photovoltaic systems. Baschel et al. (2018) study the impact of component reliability on large-scale photovoltaic system's performance. Cristaldi et al. (2015) carried out the study of Markov process reliability model for photovoltaic module encapsulation failures. Quiles et al. (2020) studied the accurate sizing of residential stand-alone photovoltaic systems considering system reliability. Abdilahi et al. (2014) perform the feasibility study of renewable energy-based micro grid system in Somaliland's urban

*Corresponding author: Ibrahim Yusuf, Department of Mathematical Sciences, Bayero University, Kano, Nigeria. Email: iyusuf.mth@buk.edu.ng

centers. Chiacchio et al. (2018) carried out the study of dynamic performance evaluation of photovoltaic power plant by stochastic hybrid fault tree automaton model. Goyal et al. (2019) study the reliability, maintainability, and sensitivity analysis of physical processing unit of sewage treatment plant. Juan et al. (2016) study the reliability analysis of distribution systems with photovoltaic generation using a power flow simulator and a parallel Monte Carlo approach. Ferreira et al. (2016) analyze the reliability analyses on distribution networks with dispersed generation. Zhang et al. (2013) conducted reliability assessment of photovoltaic power systems: review of current status and future perspectives. Xu et al. (2016) analyze the copula-based slope reliability analysis using the failure domain defined by the g-Line. Singh et al. (2020) study the Reliability analysis of repairable network system of three computer labs connected with a server under 2- out-of- 3: G configuration. Yusuf et al. (2020) performed a study of reliability analysis of communication network with redundant relay station under partial and complete failure. Vijay Kumar et al. (2021) carried out the selection of optimal software reliability growth models using an integrated entropy-TOPSIS approach. Monica Rani et al. (2020) availability redundancy allocation of washing unit in a paper mill utilizing uncertain data. Martinez-Velasco and Guerra (2016) analysed the reliability of distribution systems with photovoltaic generation using a power flow simulator using Monte Carlo approach. Nautiyal et al. (2020) analyzed the reliability characteristics of k-out-of-n network using copula. Gupta et al. (2020) discussed the operational availability of generators in steam turbine system. Kumar et al. (2020) dealt with reliability assessment of a system using fuzzy set. Monila and Ashish (2020) analyzed the performance of evaporation unit in sugar industry.

The authors investigated a number of systems linked to solar photovoltaic systems. When utilizing k-out-of-n: systems, they often have not given much attention to their operations, which may be witnessed in a number of real-world circumstances. However, we observe redundancy in subsystems, notably solar panels, in numerous sites such as banks, industries, schools, and other communication channels. In light of this exceptional architecture, we analyzed this home-based small-sized photovoltaic, with redundancy in the solar panels and batteries alone. This is due to a lack of electricity and an increase in the electric rate in our villages, which have limited resources. The configuration is serial parallel with a k-out-of-n: G operation scheme. The system exists in three states: perfect, degraded, and failing. When there are k great states in the system, the entire system is operational; nevertheless, when there are fewer than k good customers, the system is on the edge of collapsing altogether. The failure of the primary panel is regarded as a partial failure, but the failure of the redundant panels is regarded as a complete failure before the primary ones are fixed. Copula repair is used to swiftly restore the system when the charge controller and inverter switches are utilized in the system update. The system was assessed using the supplemental variable approach for different values of failure and repair rates, and various reliability indices were obtained.

2. Materials and Methods

This research focuses on the assessment of photo-voltaic simulation component flaws. The purpose of this study is to enhance and establish an optimum size of the photo-voltaic system from an economic aspect while imposing certain limits pertinent to the system's needed reliability. The goal of building a photo-voltaic producing system is to achieve maximum supply reliability. To evaluate the effectiveness of the indicated approach, the numerical data were examined in order to establish essential assumptions about the photo-voltaic device design process. The Gumbel–Hougaard copula family was used to provide formulations of system dependability measures such as reliability, mean time to failure (MTTF), availability, and profit function. Numerical examples are provided to demonstrate the acquired conclusions and to investigate the influence of various system features.

3. Description of the System and its Assumptions

(i) Description of the System

This section provides a quick overview of the photovoltaic system plant and its subsystems. Photovoltaic systems are made up of five major components: photovoltaic modules, controllers, batteries, inverters, and distribution boards. All of the components are connected in series as presented in Figure 1.

Figure 1
System reliability block diagram

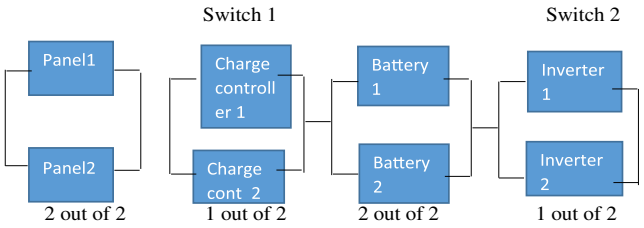

(a) Subsystem R (solar module)
There are two solar panel units linked in series to the next unit. One is in use while the other is in standby mode. The failure of the two components results in the breakdown of the entire system.

(b) Subsystem S (charge controller)
There is one charge controller unit that is linked in series to the next unit. This unit's failure results in the collapse of the entire system.

(c) Subsystem T (battery)
This subsystem has two units of batteries that are linked in series to the other subsystem. One is in use while the other is in standby mode. When this unit fails, the entire system fails.

(d) Subsystem U (inverter)
It is made up of one inverter unit. Because it is connected in series to the next unit, the failure of this unit causes the entire system to fail.

3.1. Failure Rate

The rate of failure is calculated using failures per unit time. It is calculated as the ratio of the number of items that failed throughout the testing period.

Repair rate: The repair rate is calculated using repairs per unit hour. It is calculated by dividing the number of repairs performed on the items subjected to the test period.

3.2. Mean time to Failure (MTTF)

The MTTF is defined as follows if the failure time of n items' life test information is

$$\mathrm{MTTF} = \lim_{n\to 0} \overline{P}_{up}(s).$$

3.3. Availability

Availability is a performance criterion for repairable systems that take into account both the system's reliability and durability. It is defined as the likelihood that the system will function properly when called upon. In other words, availability is the likelihood that a system will not be in a failed condition or in the midst of a repair operation when it is needed. The numerical value of availability is expressed as a probability range from 0 to 1. Estimated availability takes into account both system failures and fixes.

4. Notations and State Description

4.1. Notations

t: On a temporal scale, variable time
s: For all possible expressions, the Laplace transform variable is used
ψ_1: Subsystem 1 unit failure rate
ψ_2: Subsystem 2 unit failure rate
ψ_3: Subsystem 3 unit failure rate
ψ_4: Subsystem 4 unit failure rate
ψ_{H1}: Failure rate of subsystem 2 owing to human error
ψ_{H2}: Subsystem 2 failure rate due to human error 2
$\beta(x)$: Unit repair rate in subsystem 1
$\beta(y)$: Unit repair rate in subsystem 2
$\beta(z)$: Unit repair rate in subsystem 3
$\beta(m)$: Unit repair rate in subsystem 4
$\beta(v)$: Repair rate for subsystem 2's completely failed condition as a result of human error 1
$\beta(w)$: Repair rate for subsystem 4's completely failed condition as a result of human error 2
$p_i(t)$: The chance that the system is in the Si state at $I = 0$ to 10 instants
$\overline{P}(S)$: The probability of a state change p as transformed by Laplace (t)
$P_i(x, t)$: The likelihood that a system is in state Si for $i = 1 \ldots \ldots .8$ and the elapsed repair time is (x, t), where x represents the repair variable and t represents the time variable
$P_i(y, t)$: The probability that a system is in state Si for $i = 1 \ldots \ldots .8$ and the elapsed repair time for the system under repair is (y, t), where y is the repair variable and t is the time variable
$E_p(t)$: Profitability is anticipated during the time period $[0, t]$.
K_1, K_2: Revenue and per-unit-hour service costs are calculated separately

The elapsed repair time for the system under repair is (y, t), where y is the repair variable and t is the time variable.

5. Description and Assumptions

State	Description
S_0	Units A1 and A2 are operational in their initial form. And the system is fully working. Unit B1 in subsystem 2 is operational. Units C1 and C2 are operational in subsystem 3, while B2 is on hot standby in the second subsystem.
S_1	Unit B1 has failed and is being repaired in this state. In addition, the total repair time is (x, t). T1 is active, with B2, A1, A2, C1, C1, and D1 on standby and D2 on standby.
S_2	The D1 unit has failed, while units A1, A2, B2, C1, C2, and D2 are operational. And it is in a functional state.
S_3	S_3 is a totally failed state triggered by subsystem 1's failure.
S_4	S_4 is a totally failed state induced by the failure of two subsystem 2 units.
S_5	S_5 is a completely failed condition caused by the breakdown of a unit in subsystem 3.
S_6	S_6 is a utterly failed condition caused by the failure of two units in subsystem 4.

5.1. Assumptions

The following assumptions are used throughout the model's explanation:

(1) Initially, all subsystems are in a fine working condition.
(2) For operational mode, two units from subsystem 1 and two units from subsystem 3 must be used consecutively.
(3) For operational mode, just one unit in subsystem 2 is required. In addition, one unit out of one in subsystem 4 is required for operational mode.
(4) If one of the components in subsystem 1 fails, the system becomes unusable, and also, if one of the subsystem 3 components fails.
(5) The system will also be rendered inoperable if all two components from subsystems 2 and 4 fail.
(6) A system's failing unit can be fixed when it is in an inoperable or failed state. Copula maintenance is required once a unit in a subsystem fails completely. It is thought that a copula-repaired system performs similarly to a new system and that no damage occurs during the repair process.
(7) Once the faulty unit has been fixed, it is ready to execute the task.
(8) The failure of any of the human operators renders the system inoperable.

5.2. Formulation and Solution of Mathematical Model

Based on the probability, the following set of difference-differential equations is linked to the previous mathematical model of factors, as well as the continuity of argumentation used Nelson's (2006), the system of difference-differential equations derived from Figure 2 is provided in Singh et al. (2020).

Figure 2
Model state transition diagram

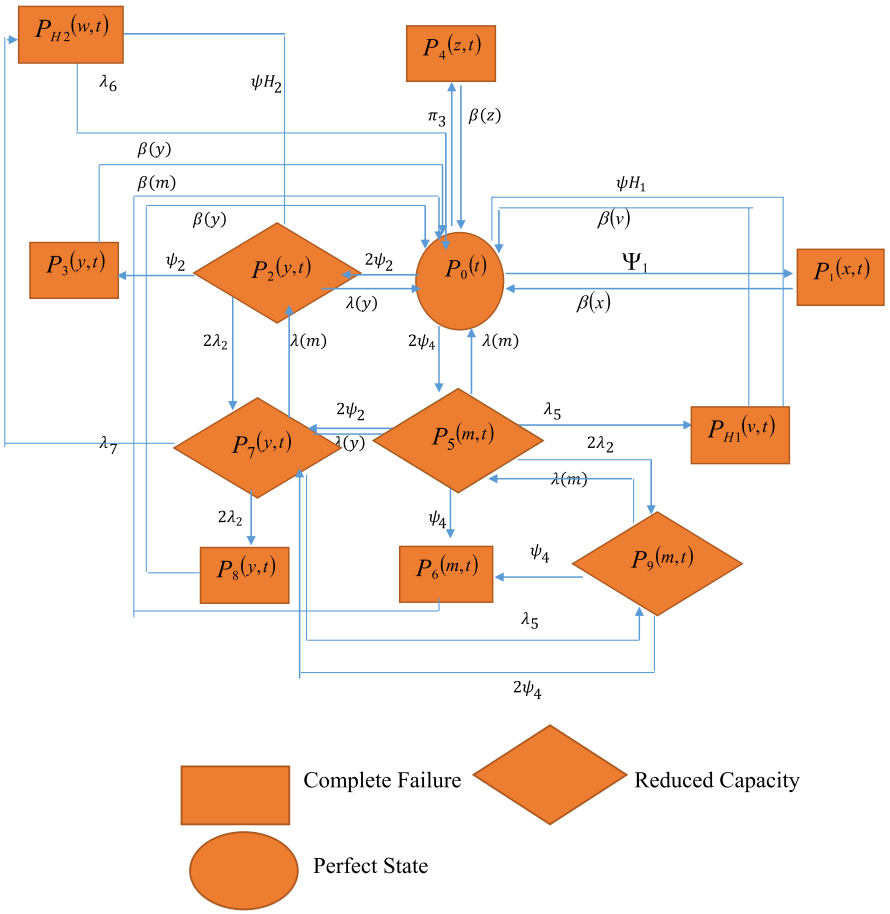

$$\left[\frac{\partial}{\partial t}+\psi_1+2\psi_1+\psi_3+2\psi_4+\psi_{H1}+\psi_{H1}\right]P_0(t) = \int_0^\infty \beta(x)P_1(x,t)dx+\int_0^\infty \lambda(y)P_2(y,t)dy+\int_0^\infty \beta(z)P_4(z,t)dz + \int_0^\infty \lambda(m)P_5(m,t)dm+\int_0^\infty \beta(v)P_{H1}(v,t)dv + \int_0^\infty \beta(w)P_{H2}(w,t)dw \quad (1)$$

$$\left[\frac{\partial}{\partial t}+\frac{\partial}{\partial x}+\beta(x)\right]P_1(x,t)=0 \quad (2)$$

$$\left[\frac{\partial}{\partial t}+\frac{\partial}{\partial y}+\psi_2+2\psi_4+\lambda_6+\lambda(y)\right]P_2(y,t)=0 \quad (3)$$

$$\left[\frac{\partial}{\partial t}+\frac{\partial}{\partial y}+\beta(y)\right]P_3(y,t)=0 \quad (4)$$

$$\left[\frac{\partial}{\partial t}+\frac{\partial}{\partial z}+\beta(z)\right]P_4(z,t)=0 \quad (5)$$

$$\left[\frac{\partial}{\partial t}+\frac{\partial}{\partial m}+\psi_4+2\psi_2+\lambda_5+\lambda(m)\right]P_5(m,t)=0 \quad (6)$$

$$\left[\frac{\partial}{\partial t}+\frac{\partial}{\partial m}+\beta(m)\right]P_6(m,t)=0 \quad (7)$$

$$\left[\frac{\partial}{\partial t}+\frac{\partial}{\partial y}+\psi_4+\lambda_7+\lambda(m)+\lambda(y)\right]P_7(y,t)=0 \quad (8)$$

$$\left[\frac{\partial}{\partial t}+\frac{\partial}{\partial y}+\beta(y)\right]P_8(y,t)=0 \quad (9)$$

$$\left[\frac{\partial}{\partial t}+\frac{\partial}{\partial v}+\beta(v)\right]P_{H1}(v,t)=0 \quad (10)$$

$$\left[\frac{\partial}{\partial t}+\frac{\partial}{\partial w}+\beta(w)\right]P_{H2}(w,t)=0 \quad (11)$$

BOUNDARY CONDITIONS

$$P_1(0,t)=\psi_1P_0(t) \quad (12)$$

$$P_2(0,t)=2\psi_2P_0(t) \quad (13)$$

$$P_3(0,t)=2\psi_2^2P_0(t) \quad (14)$$

$$P_4(0,t)=\psi_3P_0(t) \quad (15)$$

$$P_5(0,t)=2\psi_4P_0(t) \quad (16)$$

$$P_6(0,t)=2\psi_4^2P_0(t) \quad (17)$$

$$P_7(0,t)=8\psi_2\psi_4P_0(t) \quad (18)$$

$$P_8(0,t)=8\psi_2\psi_4^2P_0(t) \quad (19)$$

$$P_{H1}(0,t)=\psi_{H1}(P_0(t)+P_2(0,t)+P_5(0,t)+P_7(0,t)) \quad (20)$$

$$P_{H2}(0,t)=\psi_{H2}(P_0(t)+P_2(0,t)+P_5(0,t)+P_7(0,t)) \quad (21)$$

And the initial condition $P_0(0) = 1$, and all other probabilities of transition are zeros at t = 0.

Applying Laplace transformations of (1) to (21), we obtained the following:

$$\begin{aligned}&[s+\psi_1+2\psi_1+\psi_3+2\psi_4+\psi_{H1}+\psi_{H1}]\overline{P}_0(s)\\&=\int_0^\infty \beta(x)\overline{P}_1(x,s)dx+\int_0^\infty \lambda(y)\overline{P}_2(y,s)dy+\int_0^\infty \beta(z)\overline{P}_4(z,s)dz\\&+\int_0^\infty \lambda(m)\overline{P}_5(m,s)dm+\int_0^\infty \beta(v)\overline{P}_{H1}(v,s)dv\\&+\int_0^\infty \beta(w)\overline{P}_{H2}(w,s)dw\end{aligned} \tag{22}$$

$$\left[s+\frac{\partial}{\partial x}+\beta(x)\right]\overline{P}_1(x,s)=0 \tag{23}$$

$$\left[s+\frac{\partial}{\partial y}+\pi_2+2\pi_4+\lambda_6+\lambda(y)\right]\overline{P}_2(y,s)=0 \tag{24}$$

$$\left[s+\frac{\partial}{\partial y}+\beta(y)\right]\overline{P}_3(y,s)=0 \tag{25}$$

$$\left[s+\frac{\partial}{\partial z}+\beta(z)\right]\overline{P}_4(z,s)=0 \tag{26}$$

$$\left[s+\frac{\partial}{\partial m}+\psi_4+2\psi_2+\lambda_5+\lambda(m)\right]\overline{P}_5(m,s)=0 \tag{27}$$

$$\left[s+\frac{\partial}{\partial m}+\beta(m)\right]\overline{P}_6(m,s)=0 \tag{28}$$

$$\left[s+\frac{\partial}{\partial y}+\psi_4+\lambda_7+\lambda(m)+\lambda(y)\right]\overline{P}_7(y,s)=0 \tag{29}$$

$$\left[s+\frac{\partial}{\partial y}+\beta(y)\right]\overline{P}_9(y,s)=0 \tag{30}$$

$$\left[s+\frac{\partial}{\partial v}+\beta(v)\right]\overline{P}_{H1}(v,s)=0 \tag{31}$$

$$\left[s+\frac{\partial}{\partial w}+\beta(w)\right]\overline{P}_{H2}(w,s)=0 \tag{32}$$

LAPLACE OF THE BOUNDARY CONDITION

$$\overline{P}_1(0,s)=\psi_1\overline{P}_0(s) \tag{33}$$

$$\overline{P}_2(0,s)=2\psi_2\overline{P}_0(s) \tag{34}$$

$$\overline{P}_3(0,s)=2\psi_2^2\overline{P}_0(s) \tag{35}$$

$$\overline{P}_4(0,s)=\psi_3\overline{P}_0(s) \tag{36}$$

$$\overline{P}_5(0,s)=2\psi_4\overline{P}_0(s) \tag{37}$$

$$\overline{P}_6(0,s)=2\psi_4^2\overline{P}_0(s) \tag{38}$$

$$\overline{P}_7(0,s)=8\psi_2\psi_4\overline{P}_0(s) \tag{39}$$

$$\overline{P}_8(0,s)=8\psi_2\psi_4^2\overline{P}_0(s) \tag{40}$$

$$\overline{P}_{H1}(0,s)=\psi_{H1}(\overline{P}_0(s)+\overline{P}_2(0,s)+\overline{P}_5(0,s)+\overline{P}_7(0,s)) \tag{41}$$

$$\overline{P}_{H2}(0,s)=\psi_{H2}(\overline{P}_0(s)+\overline{P}_2(0,s)+\overline{P}_5(0,s)+\overline{P}_7(0,s)) \tag{42}$$

Solving (19) to (28) using (29) to (38) and the initial condition $P_0(0) = 1$ and using the following shifting properties of the Laplace transformation

$$\int_0^\infty \left[e^{-sx}.e^{-\int_0^x f(x)dx}\right]dx=L\left\{\frac{1-\overline{S}_f(x)}{S}\right\}=\frac{1-\overline{S}_f(x)}{S} \tag{43}$$

$$\int_0^\infty \left[e^{-sx}.f(x)e^{-\int_0^x f(x)dx}\right]dx=L\{\overline{S}_f(x)\}=\overline{S}_f(s) \tag{44}$$

we have

$$\overline{P}_1(s)=\overline{P}_1(0,s)=\left\{\frac{1-\overline{S}_\beta(s)}{S}\right\} \tag{45}$$

$$\overline{P}_2(s)=\overline{P}_2(0,s)\left\{\frac{1-\overline{S}_\lambda(s+\psi_2+2\psi_4+\lambda_6)}{S+\psi_2+2\psi_4+\lambda_6}\right\} \tag{46}$$

$$\overline{P}_3(s)=\overline{P}_3(0,s)=\left\{\frac{1-\overline{S}_\beta(s)}{S}\right\} \tag{47}$$

$$\overline{P}_4(s)=\overline{P}_4(0,s)=\left\{\frac{1-\overline{S}_\beta(s)}{S}\right\} \tag{48}$$

$$\overline{P}_5(s)=\overline{P}_5(0,s)\left\{\frac{1-\overline{S}_\lambda(s+\psi_4+2\psi_2+\lambda_5)}{S+\psi_4+2\psi_2+\lambda_5}\right\} \tag{49}$$

$$\overline{P}_6(s)=\overline{P}_6(0,s)\left\{\frac{1-\overline{S}_\beta(s)}{S}\right\} \tag{50}$$

$$\overline{P}_7(s)=\overline{P}_7(0,s)\left\{\frac{1-\overline{S}_{2\lambda}(s+\psi_4+\lambda_7)}{s+\psi_4+\lambda_7}\right\} \tag{51}$$

$$\overline{P}_8(s)=\overline{P}_8(0,s)\left\{\frac{1-\overline{S}_\beta(s)}{S}\right\} \tag{52}$$

$$\overline{P}_{H1}(s)=\overline{P}_{H1}(0,s)\left\{\frac{1-\overline{S}_\beta(s)}{S}\right\} \tag{53}$$

$$\overline{P}_{H2}(s)=\overline{P}_{H2}(0,s)\left\{\frac{1-\overline{S}_\beta(s)}{S}\right\} \tag{54}$$

Substituting the Laplace's boundary conditions, that is, (29) to (38) into (44) to (53), we have

$$\overline{P}_1(s)=\psi_1\left\{\frac{1-\overline{S}_\beta(s)}{S}\right\}\overline{P}_0(s) \tag{55}$$

$$\overline{P}_2(s)=2\psi_2\left\{\frac{1-\overline{S}_\lambda(s+\psi_2+2\psi_4+\lambda_6)}{S+\psi_2+2\psi_4+\lambda_6}\right\}\overline{P}_0(s) \tag{56}$$

$$\overline{P}_3(s)=2\psi_2^2\left\{\frac{1-\overline{S}_\beta(s)}{S}\right\}\overline{P}_0(s) \tag{57}$$

$$\overline{P}_4(s)=\psi_3\left\{\frac{1-\overline{S}_\beta(s)}{S}\right\}\overline{P}_0(s) \tag{58}$$

$$\overline{P}_5(s) = 2\psi_4\left\{\frac{1-\overline{S}_\lambda(s+\psi_4+2\psi_2+\lambda_5)}{S+\psi_4+2\psi_2+\lambda_5}\right\}\overline{P}_0(s) \quad (59)$$

$$\overline{P}_6(s) = 2\psi_4^2\left\{\frac{1-\overline{S}_\beta(s)}{S}\right\}\overline{P}_0(s) \quad (60)$$

$$\overline{P}_7(s) = 8\psi_2\psi_4\left\{\frac{1-\overline{S}_{2\lambda}(s+\psi_4+\lambda_7)}{s+\psi_4+\lambda_7}\right\}\overline{P}_0(s) \quad (61)$$

$$\overline{P}_8(s) = 8\psi_2\psi_4^2\left\{\frac{1-\overline{S}_\beta(s)}{S}\right\}\overline{P}_0(s) \quad (62)$$

$$\overline{P}_{H1}(s) = \psi_{H1}(1+2\psi_2+2\psi_4+8\psi_2\psi_4)\left\{\frac{1-\overline{S}_\beta(s)}{S}\right\}\overline{P}_0(s) \quad (63)$$

$$\overline{P}_{H2}(s) = \psi_{H2}(1+2\psi_2+2\psi_4+8\psi_2\psi_4)\left\{\frac{1-\overline{S}_\beta(s)}{S}\right\}\overline{P}_0(s) \quad (64)$$

$$\text{For } \overline{P}_0(s) = \frac{1}{D(s)} \quad (65)$$

$$\begin{aligned}\text{And } D(s) = {} & (s+\psi_1+2\psi_1+\psi_3+2\psi_4+\psi_{H1}+\psi_{H1} \\ & -[\psi_1\overline{S}_\beta(s)+2\psi_2\overline{S}_\lambda(s+\psi_2+2\psi_4+\lambda_6)+\psi_3\overline{S}_\beta(s) \\ & +2\psi_4\overline{S}_\lambda(s+\psi_4+2\psi_2+\lambda_5) \\ & +\psi_{H1}(1+2\psi_2+2\psi_4+\ 8\psi_2\psi_4)\ \overline{S}_\beta(s) \\ & +\psi_{H2}(1+2\psi_2+2\psi_4+8\psi_2\psi_4)\ \overline{S}_\beta(s)\end{aligned} \quad (66)$$

The probability that the system is working is obtained as:

$$\overline{P}_{up}(s) = \overline{P}_0(s) + \overline{P}_2(s) + \overline{P}_5(s) + \overline{P}_7(s) \quad (67)$$

By substitution

$$\begin{aligned}\overline{P}_{up}(s) = {} & \left[1+2\psi_2\left\{\frac{1-\overline{S}_\lambda(s+\psi_2+2\psi_4+\lambda_6)}{S+\psi_2+2\psi_4+\lambda_6}\right\}\right. \\ & +2\pi_4\left\{\frac{1-\overline{S}_\lambda(s+\psi_4+2\psi_2+\lambda_5)}{S+\psi_4+2\psi_2+\lambda_5}\right\} \\ & \left.+8\pi_2\pi_4\left\{\frac{1-\overline{S}_{2\lambda}(s+\psi_4+\lambda_7)}{s+\psi_4+\lambda_7}\right\}\right]\overline{P}_0(s)\end{aligned} \quad (68)$$

Equation (68) can also be interpreted by applying (65) as (69) below:

$$\begin{aligned}\overline{P}_{up}(s) = {} & \frac{1}{D(s)}\left[1+2\pi_2\left\{\frac{1-\overline{S}_\lambda(s+\pi_2+2\pi_4+\lambda_6)}{S+\pi_2+2\pi_4+\lambda_6}\right\}\right. \\ & +2\pi_4\left\{\frac{1-\overline{S}_\lambda(s+\pi_4+2\pi_2+\lambda_5)}{S+\pi_4+2\pi_2+\lambda_5}\right\} \\ & \left.+8\pi_2\pi_4\left\{\frac{1-\overline{S}_{2\lambda}(s+\pi_4+\lambda_7)}{s+\pi_4+\lambda_7}\right\}\right]\end{aligned} \quad (69)$$

$$\overline{P}_{up}(s) = 1 - \overline{P}_{down}(s) \quad (70)$$

6. Results

6.1. Formulation and Analysis of System Availability

Taking $S_{\alpha_0}(s) = \overline{S}_{\exp[x^\theta+\{\log\varphi(x)\}^\theta]^{1/\theta}}(s) = \frac{\exp[x^\theta+\{\log\varphi(x)\}^\theta]^{1/\theta}}{s+\exp[x^\theta+\{\log\varphi(x)\}^\theta]^{1/\theta}}$, $\overline{P}_\phi(s) = \frac{\phi}{s+\phi}$ *but* $\phi = 1$ and $\psi_1 = 0.001$, $\psi_2 = 0.002$, $\psi_3 = 0.003$, $\psi_4 = 0.004$, $\psi_5 = 0.005$, $\psi_6 = 0.006$, $\psi_7 = 0.007$, $\psi_{H1} = 0.008$, $\psi_{H2} = 0.009$, and repair rates $\lambda(y) = \lambda(m) = \beta(x) = \beta(y) = \beta(z) = \beta(v) = \beta(w) = \beta(m) = 1$ in equation (69), and applying the inverse Laplace transform to (69), the expression for system availability is

$$\begin{aligned}\overline{P}_{up}(t) = {} & \{\ -0.00004904770570\ e^{-1.011000000\ t} + 0.001603099809\ e^{-2.722649460\ t} \\ & +(-0.006078301855 - 0.001417810992\ I)\ e^{(-1.014501644-0.0009938111316\ I)\ t} \\ & +(-0.006078301855 + 0.001417810992\ I)\ e^{(-1.014501644+0.0009938111316\ I)\ t} \\ & +1.010602552\ e^{-0.02864725083\ t}\ \}\end{aligned} \quad (71)$$

Taking $t = 0, 10, \ldots, 100$, availability of the system is obtained and presented in Table 1.

Table 1
Availability variation in relation to time

Time (in days)	$\overline{P}_{up}(t)$
0	1.0000000
10	0.8588684
20	0.6698404
30	0.5278978
40	0.4213117
50	0.3412752
60	0.2811751
70	0.1860466
80	0.1121580
90	0.0867116
100	0.0676034

6.2. Formulation and Analysis of Reliability

Letting all repair rates $\lambda(y) = \lambda(m) = \beta(x) = \beta(y) = \beta(z) = \beta(v) = \beta(w) = \beta(m) = 0$ in equation (69) and taking the values of failure rates and employing inverse Laplace transformation, the expression is reliability relation:

$$\begin{aligned}R(t) = {} & \{\ 0.002909090909\ e^{-0.01100000000\ t} + 0.2352941176\ e^{-0.01600000000\ t} \\ & +0.3617967914\ e^{-0.03300000000\ t} + 0.4000000000\ e^{-0.01300000000\ t}\ \}\end{aligned} \quad (72)$$

Taking $t = 0, 10 \ldots 100$ and units of time in equation (72), reliability is computed and presented in Table 2.

Table 2
Variation of reliability relative to time

Time (in days)	Reliability
0	0.9999999
10	0.9144528
20	0.7586088
30	0.6729452
40	0.5603993
50	0.4857043
60	0.3749117
70	0.2650407
80	0.2108273
90	0.1295368
100	0.0908303

6.3. Formulation and Analysis of Mean Time to Failure

Setting repairs to zero equation (69), the expression for MTTF is defined as follows:

$$MTTF = \lim_{s \to 0} \overline{P}_{up}(s) \tag{73}$$

Fixing $\pi_1 = 0.001$, $\pi_2 = 0.002$, $\pi_3 = 0.003$, $\pi_4 = 0.004$, $\lambda_5 = 0.005$, $\lambda_6 = 0.006$, $\lambda_7 = 0.007$, $\pi_{H1} = 0.008$, $\pi_{H2} = 0.009$, varying π_k in equation (60), MTTF is computed with respect to failure rate as presented in Table 3.

6.4. Cost analysis

The expression for the expected profit incurred in $[0, t)$

$$E_p(t) = K_1 \int_0^t P_{up}(t)dt - K_2 t \tag{74}$$

Taking fixed values of parameters of equation (69), equation (74) follows:

$$E_p(t) = k_1 \left\{ \begin{array}{l} -0.018340e^{-2.87072t} + 0.008479e^{-1.20122t} \\ +0.000094e^{-1.15618t} - 598.072776e^{-0.00016t} \\ +0.000183e^{-1.13000t} + 0.000237e^{-1.12000t} \\ +5985.0821 \end{array} \right\} - k_2(t) \tag{75}$$

$$E_p(t) = K_1 \begin{array}{l} \{ \ 0.00004851405114\ e^{-1.011000000\ t} - 0.0005888013983\ e^{-2.722649460\ t} + (0.005992779757\ \} \\ +0.001391673744\ I)\ e^{(-1.014501644 - 0.0009938111316\ I)\ t} + (0.005992779757 \\ -0.001391673744\ I)\ e^{(-1.014501644 + 0.0009938111316\ I)\ t} - 35.27747071\ e^{-0.02864725083} \end{array}$$

Supposing $K_1 = 1$ and $K_2 = 0.1,\ 0.2 \ldots,\ 0.5$, respectively, and varying $t = 0,\ 10,\ 20 \ldots 100$ and units of time, the expected profit calculations are shown in Table 4.

7. Discussion

The simulation in Figure 3 shows how availability diminishes over time. The graph clearly shows that when the period span is 40 days or less, the system's availability is higher. Figure 4 depicts the system's dependability over time in the same manner. The graph illustrates how reliability falls from 0 to 100 as time t rises. In contrast, the time interval has a higher level of consistency. According to Figures 3 and 4, increasing the number of units on standby can improve system availability and reliability by performing perfect repair in the event of an incomplete failure, replacing the afflicted subsystem with a new one in the event of a full failure, performing frequent inspection and preventative maintenance, hiring more repair equipment, and so on.

Figure 5 shows a simulation of the mean time to failure versus the failure rate ψ_k. The graph shows that as ψ_k increases, the MTTF decreases. As ψ_k in increases, the MTTF falls, reducing the system's lifetime. It is worthwhile to include fault-tolerant components to increase the MTTF and lifespan of the system. Figure 6 shows the relationship between profit and time t for $K_2 \in \{0.01, 0.02, 0.03, 0.04, 0.05\}$. For whatever value of K_2, the anticipated profit decreases with increasing time, according to the graph. However, when the value falls, the projected profit rises.

Table 3
The relationship between MTTF and failure rates π_k

	MTTF								
Failure rate	(a)	(b)	(c)	(d)	(e)	(f)	(g)	(h)	(i)
0.001	56.9152	71.6736	56.3291	54.9259	61.2032	54.6369	53.1268	67.1616	69.8481
0.002	55.0353	62.3643	54.5688	53.8916	58.5096	54.1778	53.0621	64.6741	67.1616
0.003	54.0343	55.3235	52.9152	53.1502	56.3057	53.7893	53.0159	62.3643	64.6741
0.004	53.9222	49.7917	51.3589	52.9152	54.4692	53.4563	52.9813	60.2138	62.3643
0.005	51.7081	45.3194	49.8915	52.3446	52.9152	53.1677	52.9544	58.2067	60.2138
0.006	50.4000	41.6224	48.5056	51.5509	51.5832	52.9152	52.9328	56.3291	58.2067
0.007	47.0051	38.5112	47.1946	50.6130	50.4288	52.6924	52.9152	54.5688	56.3291
0.008	45.5300	35.8545	45.9527	49.5864	49.4187	52.4943	52.9005	52.9152	54.5688
0.009	42.98055	33.55796	44.77443	48.50983	48.52746	52.31715	52.88811	51.35890	52.91523

Table 4
Profitability as a function of time

	$E_P(t)$								
Failure rate	(a)	(b)	(c)	(d)	(e)	(f)	(g)	(h)	(i)
0.001	2184.386	−10829.17	−1817.068	1403.635	−2992.89	−500.8765	−77.575	−2583.1	−2793.92
0.002	2057.783	−8010.954	−1705.276	571.790	−2424.24	−420.8765	−53.87205	−2395.3	−2583.14
0.003	1941.875	−6192.320	−1603.492	−18.98787	−2003.50	−358.6157	−39.57946	−2227.299	−2395.33
0.004	1835.491	−4944.079	−1510.556	−424.878	−1683.50	−309.2145	−30.30303	−2076.341	−2227.29
0.005	1737.616	−4046.802	−1425.471	−697.728	−1434.46	−269.3602	−23.94313	−1940.225	−2076.34
0.006	1647.366	−3378.247	−1347.378	−876.733	−1236.85	−236.7424	−19.39393	−1817.068	−1940.22
0.007	1563.969	−2865.639	−1275.531	−989.913	−1077.44	−209.7095	−16.02804	−1705.27	−1817.06
0.008	1486.748	−2463.305	−1209.281	−1056.969	946.9696	−187.0557	−13.46801	−1603.4	−1705.27
0.009	1415.108	−2141.319	−1148.062	1091.715	−838.838	−167.8838	−11.47570	−1510.5	−1603.49

Figure 3
Availability as a time function

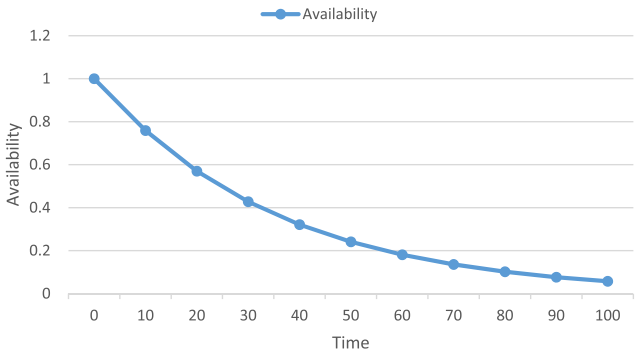

Figure 4
Reliability as a function of time

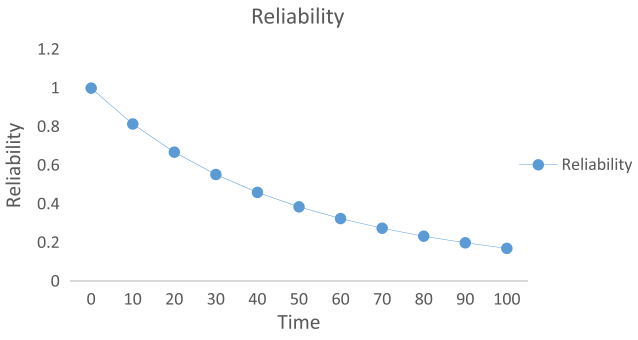

Figure 5
Variation of MTTF with failure rates

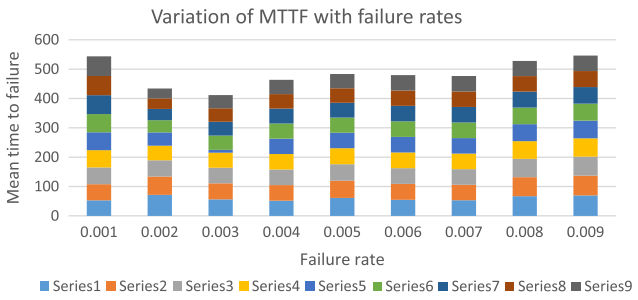

Figure 6
Expected profit against time

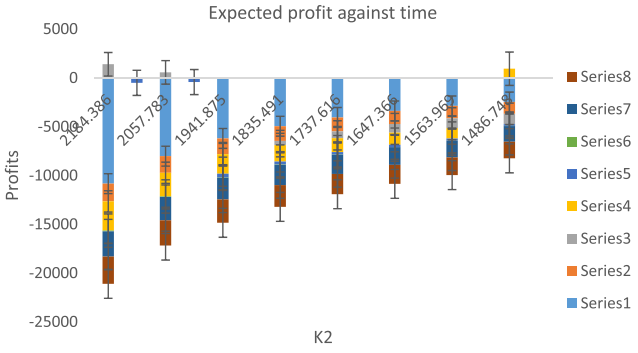

Implementing the above-mentioned replacement and redundancy ideas will improve the projected profit.

8. Conclusion

From the analysis, it is observed that the system's dependability is significantly more susceptible to the simultaneous failure rate of one solar panel and one battery unit. The model studied the dependability measures and the sensitivity analysis for a solar installation work system. The results show that system reliability is more susceptible to system failure rates, whereas system MTTF is more subject to subsystem failure rates. From the model, which consists of *n* parallel units with a standby unit, one can conclude that as a result of unit failure, catastrophic failure, and standby unit failure, the considered system's dependability is more susceptible in terms of battery and charge controller failure. The system's MTTF is shown to be equally sensitive to the failure rate of the charge controller and the system's distributor. The research is limited to a simple system with redundancy in the charge controller and inverter alone, the standby is of one unit only for each. Also, switches are employed in order to enhance the system's reliability.

Acknowledgement

We acknowledged the Sokoto State University, Sokoto for rendering support to our research.

References

Abdilahi, A. M., Abdul, H. M. Y., Mohd, W. M., Omar, T. K., Alshammari, F. S., & Faizah, M. N. (2014). Feasibility study of renewable energy-based micro grid system in Somaliland's urban centers. *Renewable and Sustainable Energy Reviews 40*, 1048–1059. https://doi.org/10.1016/j.rser.2014.07.150.

Baschel, S., Koubli, E., Roy, J., & Gottschalg, R. (2018). Impact of component reliability on large scale photovoltaic systems' performance. *Energies*, *11*, 1579. https://doi.org/10.3390/en11061579.

Chiacchio, F., Famoso, F., D'Urso, D., Brusca, S., Aizpurua, J. I., & Cedola, L. (2018). Dynamic performance evaluation of photovoltaic power plant by stochastic hybrid fault tree automaton model. *Energies*, *11*, 306. https://doi.org/10.3390/en11020306.

Cristaldi, L., Khalil, M., Faifer, M., & Soulatiantork, P. (2015, November 22-25). *Markov process reliability model for photovoltaic module encapsulation failures* [Paper presentation]. 2015 International Conference on Renewable Energy Research and Applications, Palermo, Italy. https://doi.org/10.3390/ICRERA.2015.7418696

Fashina, A. A., Akiyode, O. O., & Sanni, D. M. (2018). The status quo of rural and renewable energy development in Liberia: Policy and implementation. *SPC Journal of Energy*, *1*(1), 9–20. http://doi.org/10.14419/e.v1i1.14518.

Ferreira, H., Faas, H., Fulli, G., Kling, W. L., & Peças Lopes, J. (2016). *Reliability analyses on distribution networks with dispersed generation: A review of the state of the art* [Paper presentation]. Powergrid 2010 Proceedings, Tulsa, USA. https://publications.jrc.ec.europa.eu/repository/handle/JRC56614

Garg, H., Rani, M., & Sharma, S. P. (2013). Reliability analysis of the engineering systems using intuitionistic fuzzy set theory. *International Journal of Quality and Reliability Engineering*, Article 943972. http://dx.doi.org/10.1155/2013/943972.

Goyal, D., Kumar, A., Saini, M., & Joshi, H. (2019). Reliability, maintainability and sensitivity analysis of physical processing unit of sewage treatment plant. *SN Applied Sciences*, *1*, Article 1507. https://doi.org/10.1007/s42452-019-1544-7.

Gupta, N., Saini, M., & Kumar, M. A. (2020). Operational availability analysis of generators in steam turbine power plants. *SN Applied Sciences*, *2*(4), 779–790. https://doi.org/10.1007/s42452-020-2520-y.

Kumar, V., Saxena, P., & Garg, H. (2021). Selection of optimal software reliability growth models using an integrated entropy–Technique for Order Preference by Similarity to an Ideal Solution (TOPSIS) approach. *Mathematical Methods in the Applied Sciences*. http://doi.org/10.1002/mma.7445.

Kumar, A., Singh, S.B., & Ram, M. (2020). Systems reliability assessment using hesitant fuzzy set. *International Journal of Operational Research*, *38*(1), 1–18. http://doi.org/10.1504/IJOR.2020.106357.

Martinez-Velasco, J. A., & Guerra, G. (2016). Reliability analysis of distribution systems with photovoltaic generation using a power flow simulator and a parallel Monte Carlo approach. *Energies 9*(7), 537. http://doi.org/10.3390/en9070537.

Monika Rani, M., Sharma, S. P., & Garg, H. (2020). Availability redundancy allocation of washing unit in a paper mill utilizing uncertain data. *Elixir Mechanical Engineering*, *39C*, 4627–4630, 20. https://www.elixirpublishers.com/articles/1350640878_39%20C%20(2011)%204627-4631.pdf

Monika, S., & Ashish, K. (2019). Performance analysis of evaporation system in sugar industry using RAMD analysis. *Journal of Brazilian Society of Mechanical Science and Engineering*, *41*, Article 175. https://doi.org/10.1007/s40430-019-1681-3.

Nautiyal, N., Singh, S. B., & Bisht, S. (2020). Analysis of reliability and its characteristics of a k-out-of-n network incorporating copula. *International Journal of Quality Reliability and Management*, *37*(4), 517–537. https://doi.org/10.1108/IJQRM-08-2018-0224.

Nelson, R.B. (2006). *An Introduction to Copulas*, 2nd ed. Springer.

Patelli, E., & Beer, M. (2017). *Reliability analysis on complex systems with common cause failures* [Paper presentation]. 12th International Conference on Structural Safety and Reliability, Vienna, Austria. https://www.researchgate.net/publication/319077308_Reliability_Analysis_on_Complex_Systems_with_Common_Cause_Failures

Quiles, E., Roldán-Blay, C., Escrivá-Escrivá, G., & Roldán-Porta, C. (2020). Accurate sizing of residential stand-alone photovoltaic systems considering system reliability. *Sustainability*, *12*(3), 1274. http://doi.org/10.3390/su12031274.

Rengasamy, M., Gangatharan, S., Elavarasan, R. M., & Mihet-Popa, L. (2020). The Motivation for incorporation of microgrid technology in rooftop solar photovoltaic deployment to enhance energy economics. *Sustainability*, *12*, 10365. http://doi.org/10.3390/su122410365.

Salah, J. A., & Fashina, A. A. (2019). Design of a hybrid solar photovoltaic system for Gollis University's administrative block, Somaliland. *International Journal of Physical Research*, *7*(2): 37–47. http://doi.org/10.14419/ijpr.v7i2.28949.

Sayed, A., El-Shimy, M., El-Metwally, M., & Elshahed, M. (2019). Reliability, availability and maintainability analysis for grid-connected solar photovoltaic systems. *Energies*, *12*, 1213. http://doi.org/10.3390/en12071213.

Singh, V. V., Poonia, P. K., & Abdullahi, A. F. (2020). Performance analysis of a complex repairable system with two subsystems in series configuration with an imperfect switch. *Journal of Mathematics and Computational Science*, *10*(2), 359–383. https://doi.org/10.28919/jmcs/4399.

Uswarman, R., & Rushdi, A. M. (2021). Reliability evaluation of rooftop solar photovoltaic using coherent threshold systems. *Journal of Engineering Research and Reports*, *20*(2), 32–44. https://doi.org/10.9734/jerr/2021/v20i217263.

Xu, X., Jianlin, L., Gong, J., Deng, H., & Wan, L. (2016). Copula-based slope reliability analysis using the failure domain defined by the g-line. *Mathematical Problems in Engineering*, Article 6141838. http://dx.doi.org/10.1155/2016/6141838.

Yusuf, I., Ismail, A. L., & Ali, U. A. (2020). Reliability analysis of communication network with redundant relay station under partial and complete failure. *Journal of Mathematics and Computer Science*, *10*(4), 863–880. https://doi.org/10.28919/jmcs/4408.

Zhang, P., Li, W., Li, S., Wang, Y., & Xiao, W. (2013). Reliability assessment of photovoltaic power systems: Review of current status and future perspectives. *Applied Energy*, *104*, 822–833. https://doi.org/10.1016/j.apenergy.2012.12.010.